SPi	Journal Code				Article ID				Dispatch: 16.09.16	CE: Mary Charlane Payuan
	S	I	A		6	1	7	5	No. of Pages: 7	ME:

Research article

SURFACE and INTERFACE ANALYSIS

Received: 7 July 2016 Revised: 2 September 2016 Accepted: 4 September 2016 Published online in Wiley Online Library

(wileyonlinelibrary.com) DOI 10.1002/sia.6175

Transparent hydrophobic and superhydrophobic coatings fabricated using polyamide 12–SiO_2 nanocomposite

Q2 G. Prasad,[a,b] R.P.S. Chakradhar,[a]* Parthasarathi Bera,[a] ~~A Anad~~ Prabu[b]* and C. Anandan[a]

Optically transparent hydrophobic and superhydrophobic coatings have been prepared using polyamide 12–SiO_2 nanocomposite (NC) on glass substrates by the spin-coating method. The coatings have been optimized for their hydrophobicity and transparency. The transformation from hydrophobic to superhydrophobicity is achieved with increase in roughness (R_a) which increases with SiO_2 content. These coatings are highly transparent in the entire visible region (400–800 nm). The influence of layer thickness on water contact angle (WCA) and optical transmittance of the coatings has been studied. Field emission scanning electron micrograph (FESEM) shows the presence of SiO_2 nanoparticles covered with polyamide homogenously on the surface and the particles are aggregated to form a rough structure. X-ray diffraction (XRD) patterns show that the polyamide losses its crystalline structure in the composite. The preparation procedure reported here is simple and eco-friendly. The dual nature of the coatings, that is, high transparency and superhydrophobicity in the entire visible region suggests for its potential usage in self-cleanings, wind screen and optoelectronic applications. Copyright © 2016 John Wiley & Sons, Ltd.

Keywords: polyamide 12–SiO_2; XRD; XPS; WCA; superhydrophobicity; optical transmittance

Introduction

The fabrication and study of hydrophobic and superhydrophobic surfaces/coatings have emerged as one of the most popular research topics in recent times because of its potential applications in self-cleaning, stain-resistant and ice-repellent properties.[1–4] The hydrophobicity of any surface is usually qualified with the help of water contact angle (WCA). WCA greater than 90° is refereed as hydrophobic, and if it is greater than 150° then the surface is considered as superhydrophobic in nature. The development of technology and their applications have extended to new fields such as energy efficient coatings that are both self-cleaning and transparent for potential applications in solar cells, window treatment and optical equipment, etc. The application of transparent superhydrophobic coatings on optical surfaces can improve outdoor performance via a 'self-cleaning' effect similar to the Lotus effect. Among the various coatings and materials developed so far, the clear transparent hydrophobic and superhydrophobic coatings are probably the most commercially viable and likely to produce a big impact on the society. However, developing optically transparent superhydrophobicity on glass substrates is a challenging task, because requirement for hydrophobicity typically competes with transparency. The superhydrophobic property is controlled both by its chemical nature and surface topography or roughness.[5,6] The surface features (i.e. surface roughness) associated with hydrophobicity are typically light scattering, thereby making such surfaces to appear as opaque or translucent. Hence, controlling the surface roughness to an appropriate value to obtain a transparent superhydrophobic surface is a vital process to get the desired properties. The micro- and nano-structures should be precisely tuned so that transparency and superhydrophobicity have two paradoxical requirements for the hierarchical structure.

Even though various studies have been attempted to fabricate transparent superhydrophobic surfaces,[7–13] a good balance between transparency and durability remains unsolved. Despite many theoretical and experimental efforts, inexpensive manufacturing of superhydrophobic surfaces remains problematic. As a part of our program on superhydrophobic surfaces,[14–16] we report here a simple method to prepare transparent polymer-based nanocomposite (polyamide 12–SiO_2) hydrophobic and superhydrophobic coatings. Polyamides are considered to be one of the most important super-engineering materials because of their superior mechanical properties at elevated temperatures and thermal stability, and SiO_2 is the most commonly used material for the preparation of nanocomposites.[17] In the present work, the authors are interested to prepare transparent hydrophobic and superhydrophobic coatings on glass substrates with more emphasis on transparent superhydrophobic coatings, as developing optically transparent

* *Correspondence to: R.P.S. Chakradhar, Surface Engineering Division, CSIR—National Aerospace Laboratories, Bangalore 560017, India. and ~~A Anad~~ Prabu, Centre for Nanomaterials, Department of Chemistry, School of Advanced Sciences, VIT University, Vellore 632014, India.*
E-mail: chakra@nal.res; anandprabu@vit.ac.in

a *Surface Engineering Division, CSIR—National Aerospace Laboratories, Bangalore 560017, India*

b *Centre for Nanomaterials, Department of Chemistry, School of Advanced Sciences, VIT University, Vellore 632014, India*

superhydrophobicity is challenging. The coatings have been prepared through successive spin coating of hydrophobically modified silica (HMS) dispersed onto polymer films as the spin coating is a facile method. The coatings have been characterized using X-ray diffraction (XRD), field emission scanning electron microscopy (FESEM), 3D surface profilometry, Fourier transform infrared spectroscopy (FTIR) and X-ray photoelectron spectroscopy (XPS). The influence of layer thickness on WCA and optical transmittance of the coatings have been studied by UV–Vis spectroscopy.

Experimental details

Polyamide 12 (nylon) and p-cresol were procured from S. D. Fine Chemicals, and HMS was procured from M/s ABCR GmbH, Germany. Nylon stock solution was prepared by mixing a 0.2 g of polyamide 12 with 20 ml of p-cresol, and it was magnetically stirred for 3 days under ambient condition. Around 1 g of HM silica was dispersed in 5 ml of p-cresol by ultrasonication for 30 min. The resulting colloidal suspension was mixed with as-prepared 1 wt.% polyamide 12 solution and magnetically stirred for overnight until a homogenous mixture was obtained.

Glass slides of 35 mm × 25 mm × 1 mm dimension were used as a substrate for spin coating. Before spin coating, the slide substrates were ultrasonicated in alcohol for about 10 min and then sonicated in distilled water for another 10 min. The cleaned surfaces were then subjected to spin coating. The mixture of polyamide 12 and different concentrations of HMS (0.25, 0.75, 2 and 4 wt.%) composite solution was prepared and spin coated on glass substrates with spinning speed of 3000 rpm. The coatings were optimized for their hydrophobicity and transparency on glass substrates. The coatings were dried at room temperature overnight.

XRD patterns were recorded using Bruker D8 Advance diffractometer using Cu Kα ($\lambda = 0.154178$ nm) radiation, 40-kV voltage and 40-μA current. The scanning range was $\theta = 10 - 80°$, and the scanning speed was 0.50° min^{-1}. The surface morphologies of the coatings were examined using field emission scanning electron micrograph (FESEM) (Carl Zeiss Supra 40 VP). The image analysis of the coating was carried out using the image analysis software LAS V4.6 attached to LEICA MEIREN image analyzer. The 3D roughness profiles were measured using 3D profilometer (Nano Map 500LS from AEP Technology, USA). The roughness values were measured by contact mode having a tip radius of 50 nm with a scan area of 200 μm × 200 μm. The contact force and scanning speed used were 10 mg and 200 μm s^{-1}, respectively. Static WCAs of the coatings were measured using a contact angle analyzer (Phoenix 300 Plus from M/s Surface Electro Optics, Korea). Measurements were made using tangent line-fitting mode. Water sliding angle (SA) was measured using a home-made instrument. The drop volume for WCA and SA measurements was 8 μl. Deionized Milli Q water was used for the measurements. An average of five measurements was taken for reporting of WCA, and the error in measurements was within ±2°. The optical transmission spectra were measured using UV–Vis spectrophotometer (Ocean Optics 2000, USA). FTIR studies were performed on a Shimadzu IRAffinity-1 spectrometer with KBr pellets. XPS of polyamide 12 and polyamide 12–SiO_2 coatings were recorded with a SPECS spectrometer using non-monochromatic AlKα radiation (1486.6 eV) as an X-ray source operated at 150 W (12 kV, 12.5 mA). The binding energies reported here were referenced with C1s peak at 284.6 eV. Survey spectra were obtained with pass energy of 70 eV whereas individual spectra were recorded with 40-eV pass energy with 0.05-eV step increment.

Results and discussion

XRD studies

From **Fig**. 1, it can be observed that the water droplet retains its spherical shape on the coated glass. Further, the letters underneath the coated glass can clearly be seen indicating that the coatings are of high transparency. The XRD measurements have been used to investigate the influence of silica nanoparticles on the crystallization of polyamide 12. **Fig**ure 2 shows the XRD patterns of (a) polyamide 12 coating, (b) hydrophobically modified SiO_2 and coatings with different concentrations of polyamide 12–SiO_2 (c) (1:0.25), (d) (1:0.75), (e) (1:2) and (f) (1:4) coatings, respectively. Several crystalline structures have been defined for polyamide 12.[18] The crystal structure of polyamide depends on the crystallization conditions. It has been demonstrated that polyamide 12 shows two strong characteristic diffraction peaks around $2\theta = 20.3°$ and 21.0° which are designated as α′ and α phases of polyamide, and the crystal

Figure 1. Photograph of water droplet on the transparent and superhydrophobic polyamide 12–SiO_2 (1:4) coating on glass slide.

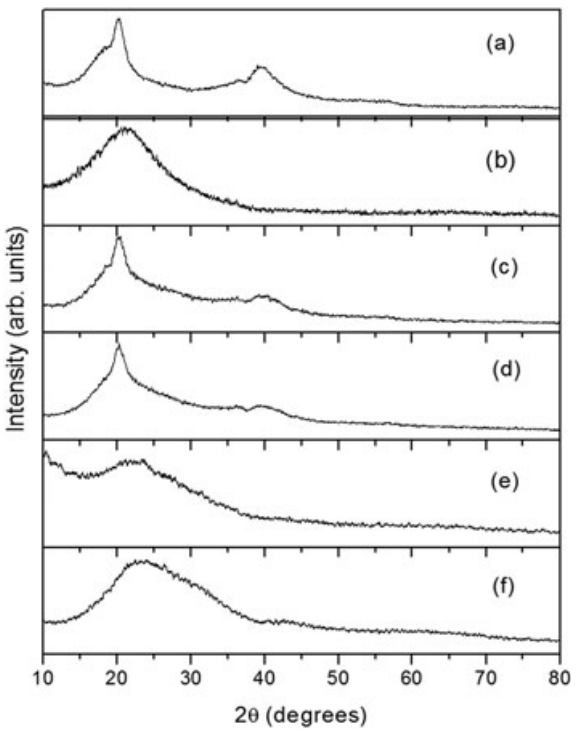

Figure 2. XRD patterns of (a) polyamide 12 coating, (b) hydrophobically modified SiO_2 (HMS) and different concentrations of polyamide 12:SiO_2 (c) (1:0.25), (d) (1:0.75), (e) (1:2) and (f) (1:4) coatings.

structure is mostly monoclinic and is believed to be a less stable phase.[19] On the contrary, if the samples are crystallized by slow cooling or by rapid quenching from the melt, then it shows γ or hexagonal phase at room temperature.[20] If the polyamide 12 is crystallized at high temperature and pressure, then it exhibits both α and γ phase at room temperature.[20–22]

In the present work, polyamide 12 [**Fig**. 2 (**a**)] shows a sharp peak at 2θ = 20.20° along with two broad peaks at 2θ = 36.59° and 39.50°. The distinct peak at 2θ = 20.20° is assigned to the α phase of polyamide 12 which is attributed to the (100) crystal planes of α crystal form. However, the origin of broad peaks at 2θ = 36.59° and 39.50° are not known. The diffraction pattern of **Fig**. 2 (**b**) indicates a broad peak at 2θ = 21. 342°, which reveals the amorphous nature of the silica nanoparticles. Music *et al.*[23] also recorded one broadened XRD peak for amorphous silica centered at the 2θ value close to the present measurement. Nallathambi *et al.*[24] observed similar diffraction pattern for silica nanoparticles. When low concentration (0.25 and 0.75 wt.%) of HMS is introduced into the polyamide 12, there is not much change in the crystallinity of the composite coating as the peak at 20.20° remains sharp. However, at higher concentrations (2 and 4 wt.%) of HMS, there is a drastic change in their XRD patterns [**Fig**. 2 (**e**, **f**)] suggesting that the addition of HMS changes the crystal form of polyamide 12. The diffraction pattern of polyamide 12–SiO_2 (2 and 4 wt.%) of the coatings exhibits a broad peak at 2θ = 23.432° on the higher 2θ side of polyamide 12 and broadness of SiO_2. Further, the full width at half maximum (FWHM) of this diffraction peak suggests the decrease in the degree of polyamide 12 crystallinity. This result indicates that the incorporation of HMS can influence crystallization of polyamide 12 and makes the microstructure of polyamide 12 amorphous.

FESEM studies

FESEM analysis has been performed to get the information on the size and distribution of the silica particles, extent of surface cover- F3 age and topography. **Fig**ure 3 shows the FESEM image of polyamide 12–SiO_2 (1:4) superhydrophobic coating. From the micrograph, it can be observed that the SiO_2 particles which are in white globular shape have been dispersed into polyamide matrix uniformly. The agglomerated particles and the size distribution have been estimated using the Leica's image analysis software LAS V4.6, and the F4 results are shown in **Fig**. 4. It can be seen from the figure that the distribution of agglomerated silica particles is skewed towards higher agglomerate size, and the size of the agglomerates is found to be <3.25 μm. However, majority (>50%) of the agglomerates are between 0.8 and 1.6 μm. As already discussed, one of the critical features to get superhydrophobicity is the presence of micro-nano sized hierarchical structures in the coating. The coating with

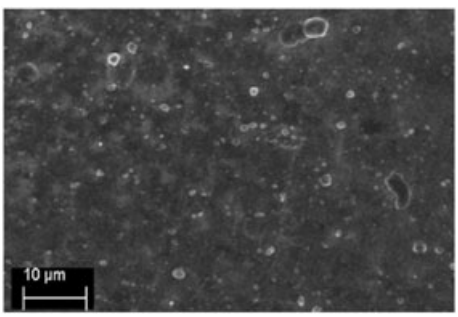

Figure 3. FESEM micrograph of polyamide 12–SiO_2 (1:4) superhydrophobic coating.

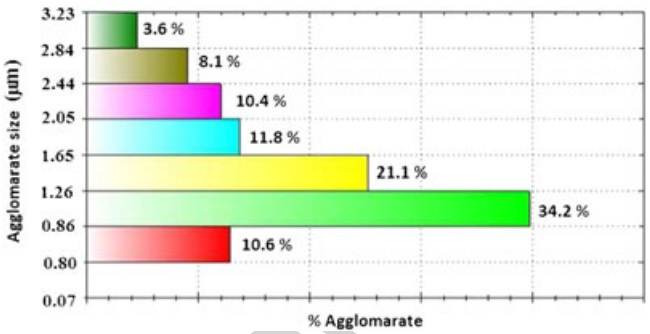

Figure 4. Distribution of agglomerated size *versus* agglomeration of silica particles in polyamide 12–SiO_2 (1:4) superhydrophobic coating.

aggregated silica particles exhibits topography with micro and nano scales suitable for entrapping air and thus generates superhydrophobic surface with high WCA. Spin coating would lead to close packed HMS because of shear induced ordering and hence helps to increase surface roughness by aggregation.[25,26]

AFM studies

Figure 5 shows the 3D roughness images of (a) polyamide 12 coat- F5 ing and different concentrations of polyamide 12:SiO_2 (c) (1:0.25), (d) (1:0.75), (e) (1:2) and (f) (1:4) coatings, respectively. The average roughness (R_a) and roughness in Z direction (R_Z) values are obtained from these images which are given in Table 1 and compared T1 with contact angle in **Fig**. 10. The surface roughness studies of the coatings reveal that polyamide 12–SiO_2 coatings have higher roughness than polyamide 12 coating. It is observed that with increase in concentration of HMS, there is a gradual increase in roughness from 88 nm to 233 nm. In order to achieve the integration of superhydrophobicity and good transparency with the same surface, the dimensions of the roughness should be lower than the wavelength of the visible light.[27]

XPS studies

Figure 6 shows the XPS survey spectra of (a) pure polyamide 12 F6 and (b) polyamide 12–SiO_2 coatings, respectively. The survey spectrum of pure polyamide 12 shows the presence of C, O and N, whereas Si is observed to be present along with C, O and N in the polyamide 12–SiO_2 coating [**Fig**. 6 (**b**)]. Presence of Si peaks in polyamide 12–SiO_2 coating indicates that SiO_2 and nylon coexist on its surface. It is observed that the amount of N is very less in polyamide 12–SiO_2 superhydrophobic coating. This can be because of the presence of SiO_2 particles on the surface.

The N1s core level spectra of pure polyamide 12 and polyamide 12–SiO_2 composite are presented in **Fig**. 7 (**a**) and (**b**) and F7 Si2p core level spectrum of polyamide 12–SiO_2 composite in **Fig**. 7 (**c**), respectively. N1s core level peak at 399.4 eV is assigned for nitrogen present in polyamide 12 that agrees well with the literature.[28] However, less intense peak at 399.2 eV observed in polyamide 12–SiO_2 coating [**Fig**. 7 (**b**)] is because of lower concentration of polyamide 12 in the composite. Si2p core level peak at 103.7 eV is attributed to SiO_2 in polyamide 12–SiO_2 coating.[29]

Relative surface concentrations of N and Si in polyamide 12–SiO_2 coating have been estimated by the relation[30]:

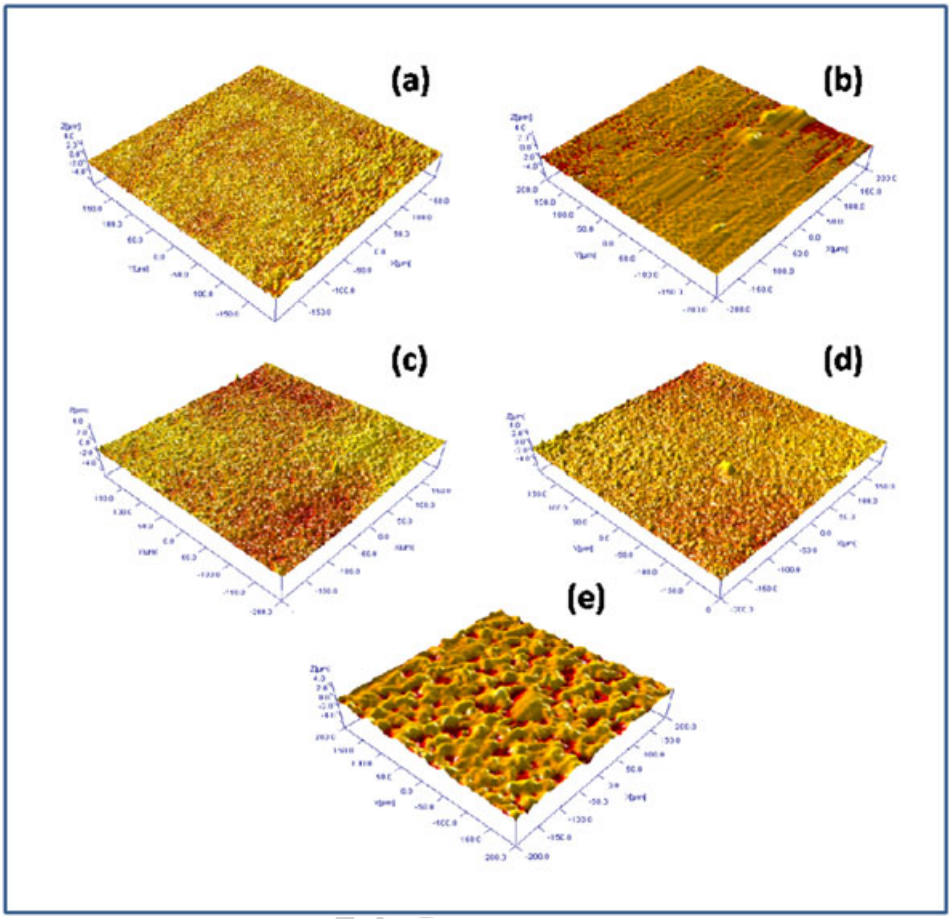

Figure 5. 3D roughness images of (a) polyamide 12 coating and different concentrations of polyamide 12:SiO_2 (b) (1:0.25), (c) (1:0.75), (d) (1:2) and (e) (1:4) coatings.

Table 1. R_a and R_z values for variable amount silica percentage in PA12: SiO_2 coatings

Polyamide12:SiO_2	R_a (nm)	R_z (nm)
1:0	88	112
1:0.25	92	121
1:0.75	129	162
1:2	173	236
1:4	233	299

$$\frac{C_N}{C_{Si}} = \frac{I_N \sigma_{Si} \lambda_{Si} D_{Si}}{I_{Si} \sigma_N \lambda_N D_N} \quad (1)$$

where C, I, σ, λ and D are the surface concentration, intensity, photoionization cross section, mean escape depth and analyzer detection efficiency, respectively. Integrated intensities of N1s and Si2p peaks have been taken into account to estimate the concentration, whereas photoionization cross sections and mean escape depths have been obtained from the literature.[31,32] The surface concentration ratio of N to Si evaluated from XPS is 0.02 in terms of atomic percentage in polyamide 12–SiO_2 coating which is in agreement with the starting batch composition (1:4) in wt.%. This shows that polyamide 12 forms a very thin coating, probably few tens of nm thick on the silica surface as a binder.

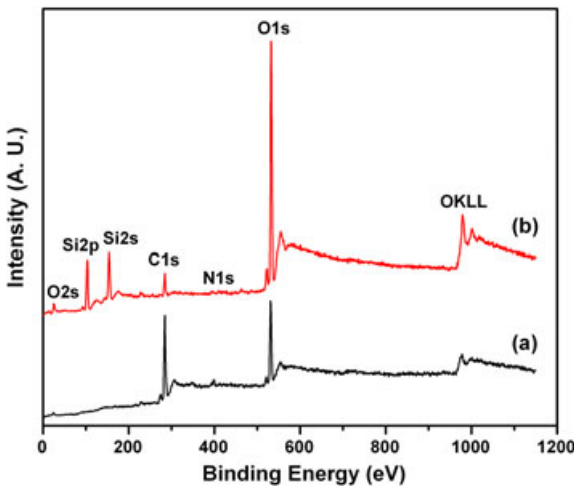

Figure 6. Survey spectra of (a) pure polyamide 12 and (b) polyamide 12–SiO_2 (1:4) transparent superhydrophobic coating.

FTIR studies

Characterization of polyamide–silica nanocomposite coatings has also been carried out with FTIR and is shown in **Fig.** 8. The spectrum exhibits characteristic absorption bands associated with both polyamide and silica. The observed peaks at 843 and 1043 cm^{-1} are attributed to Si—O bending vibration and asymmetric stretching

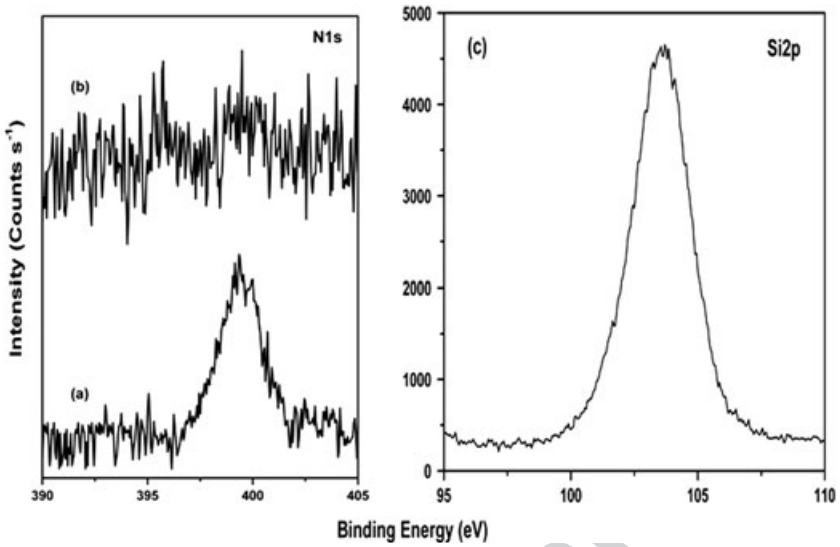

Figure 7. N1s core level spectrum of (a) pure polyamide 12, (b) polyamide 12–SiO_2 (1:4) and (c) Si2p core level spectrum of polyamide 12–SiO_2 coating.

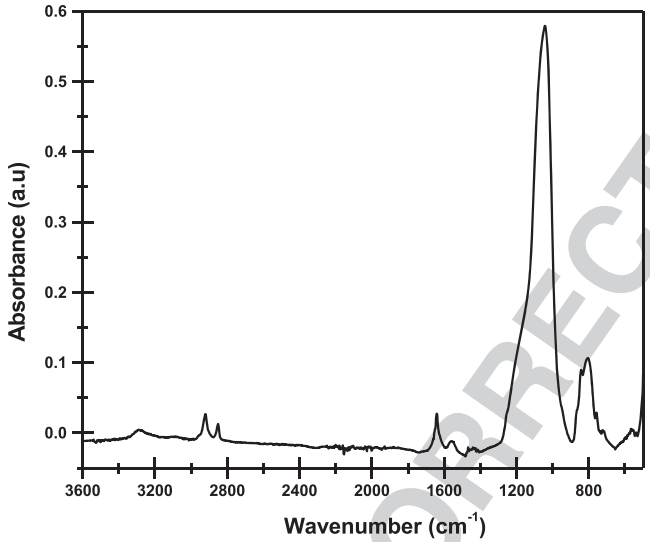

Figure 8. FTIR spectrum of polyamide 12–SiO_2 (1:4) superhydrophobic coating.

vibration of Si—O—Si bands, respectively, that corresponds to SiO_2 in the coating.[33] Further, the bands associated with CH_2 rocking type bending vibration, N—H bending, C=O stretching, symmetric vibrations of C—H, asymmetric vibrations of C—H, C—H stretching and N—H stretching are found at 716, 1549, 1641, 2851, 2920, 3089 and 3291 cm^{-1} indicating the presence of polyamide in the nanocomposite coating.[34]

Wettability studies

F9 **Figure** 9 shows the images of water droplets on (a) polyamide 12, (b) polyamide 12–SiO_2 hydrophobic and (c) polyamide 12–SiO_2 (1:4) superhydrophobic coatings on glass substrate. It is observed that the WCA of polyamide 12 is 66° which indicates hydrophilic nature with SA greater than 90°. On the other hand, with the incorporation of HMS into polyamide 12 matrix (1:2), the WCA increases to 123° exhibiting hydrophobic nature whereas further increase in HMS into polyamide 12 matrix (1:4) leads to WCA of 159° with SA less than 2° exhibiting superhydrophobicity. The correlation of roughness (R_a) and WCA with variable amount of silica content is shown in **Fig**. 10. F10

The increase in WCA with addition of HMS is because of increased roughness and the theoretical explanation on the effect of surface roughness and wetting behavior has been provided by Wenzel[35] and Cassie and Baxter.[36] When a water drop falls on a superhydrophobic surface either of two possibilities can occur, the drop may spread on the surface (Wenzel state) or it might sit on the top of the surface (Cassie state). In the Wenzel state, the apparent WCA (θ^*) on the rough surface can be related to the WCA by the relation:

$$\mathrm{Cos}\theta^* = r\,\mathrm{Cos}\theta \qquad (2)$$

where r is the roughness of the coating defined as the ratio between the true surface area by the apparent flat surface. Cassiee and Baxter have correlated the apparent contact angle (θ^*) on a rough surface to the weighted average of the cosines of the contact angles on the solid and air surfaces, where (f) is defined as the fraction of the surface on top of the protrusions, ($1-f$) the fraction of air pockets and (θ_g) the contact angle on the air in the valleys.[37] By combining the Cassie–Baxter and Wenzel relationships, a general equation can be obtained for the apparent contact angles measured on a rough surface (θ_R) which is given below:

$$\mathrm{Cos}\theta_R = \mathrm{r.f.}\cos\theta + \mathrm{f} - 1. \qquad (3)$$

As can be easily deduced from Eqn 2, increased surface roughness will lead to much higher contact angles for hydrophobic surfaces that have a contact angle $> 90°$ on flat surfaces.

In the present work, the influence of polyamide 12–SiO_2 coatings layer thickness on the WCA has also been studied. The WCA slightly varies with different thickness of coatings. It is observed that the WCA values gradually decrease with increase in the thickness. Single layer coating has 159° contact angle whereas two layers and three layers have 155° and 154° contact angles, respectively, and all the coatings exhibit SAs less than 2°. The surface free energy (γ_p) of the polyamide 12, polyamide 12–SiO_2 hydrophobic and polyamide 12–SiO_2 superhydrophobic coatings can be evaluated using the following equation:

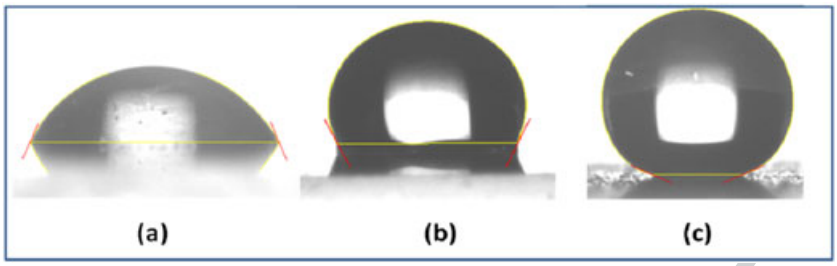

Figure 9. Water contact angle (WCA) measurements on (a) polyamide 12, (b) polyamide 12–SiO_2 (1:2) and (c) polyamide 12–SiO_2 (1:4) coatings on glass substrate.

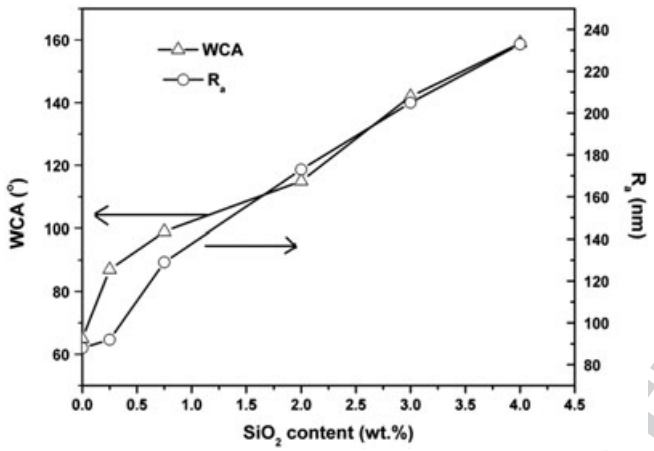

Figure 10. Variation of WCA and roughness with different wt.% of silica content.

$$\gamma p = \frac{\gamma_w (1+\cos\theta)^2}{4} \quad (4)$$

where γ_w is the surface tension of water whose value is 72.99 mN m^{-1}. The surface free energy for polyamide 12 is found to be 36.11 erg cm^{-2}. For polyamide 12–SiO_2 hydrophobic coating, the surface free energy is found to be 6.096 erg cm^{-2} whereas for single-layer, two-layer and three-layered superhydrophobic coatings, they are 0.080, 0.160 and 0.187 erg cm^{-2}, respectively. The work of adhesion (W) on such surfaces of polyamide 12 and polyamide 12–SiO_2 coatings have also been evaluated using Young–Dupre's equation[38,39]:

$$W_{sl} = \gamma_{la}(1 + \cos\theta) \quad (4)$$

where W_{sl} is the work of adhesion between solid and liquid surface and γ_{la} is the liquid–air interfacial surface tension, which is 72.99 mN m^{-1} for water. The work of adhesion for polyamide 12 coating is found to be 102.67 mN m^{-1}, for hydrophobic polyamide 12–SiO_2 (1:2) coating it is 42.18 mN m^{-1} and for the polyamide 12–SiO_2 (1:4) superhydrophobic coatings with one layer, two layers and three layers they are 4.878, 6.838 and 7.387 mN m^{-1}, respectively. As discussed earlier, the average roughness of polyamide 12–SiO_2 coatings of single layer is 180 nm. Addition of more layers may result in a slight decrease in the surface roughness. This is most probably because of the maximum coverage of surface and agglomeration of silica particles which has resulted in a slight decrease in WCA. The studies on surface free energies and work of adhesion also support the above conclusions.

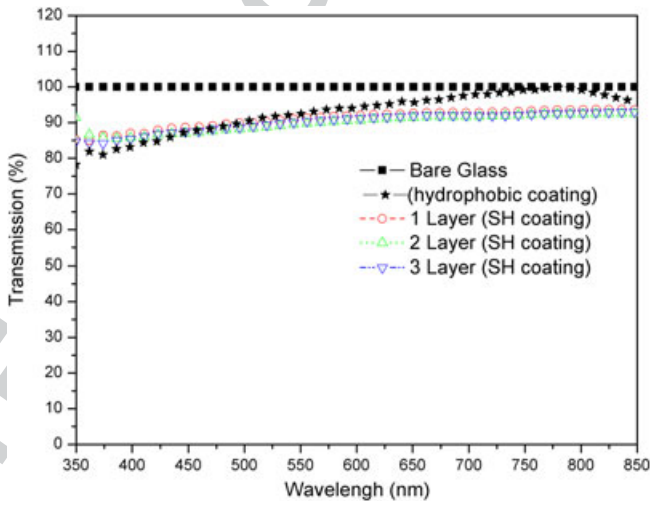

Figure 11. Transmittance of bare glass and spin coated polyamide 12–SiO_2 (1:2) hydrophobic and superhydrophobic (1:4) coatings on glass substrate.

Transmittance studies

The transmittance spectra of glass, polyamide 12–SiO_2 hydrophobic and different layers of polyamide 12–SiO_2 superhydrophobic coatings have been recorded and can be better visualized if the transmission data (T%) are plotted as in Fig. 11, $\left(\frac{T_c}{T_{glass}}\right)\times 100$, where Tc is the transmittance of the coated surface and T_{glass} is the transmittance of untreated glass slide. As in the figure, a good transparency can be seen in the entire visible region (400–800 nm). In order to get superhydrophobicity, a rough surface structure is necessary. However, this type of structure often leads to severe light scattering because of its large roughness which is comparable to or even much larger than the visible light wavelength.[40] In the present work, low enough roughness for scattering of visible light to get good optical transparency has been achieved. From the figure, it is observed that the coatings have high transmittance of 87.7% at 400 nm to 93.7% at 850 nm for superhydrophobic coatings, whereas for hydrophobic coatings it varies from 95 to 97% in the range 500 to 850 nm. The transmittance at 600 nm is around 91–93%, suggesting that these coatings can find potential applications.

Conclusions

Highly transparent hydrophobic and superhydrophobic polyamide 12–SiO_2 nanocomposite coatings have successfully been prepared by the spin coating method. The average roughness of superhydrophobic polyamide 12–SiO_2 coatings is 180 nm; addition

of more layers results in a slight decrease in the surface roughness, agglomeration of silica particles which resulted in a slight decrease in WCA. The polyamide forms a few tens of nanometer thick coating on the silica particles and binds them. XRD studies show interaction between nitrogen in the polyamide and silicon in the silica nanoparticles leading to an amorphous structure of the coating.

Acknowledgements

The authors are grateful to Director, CSIR—National Aerospace Laboratories, Bangalore, and constant support and encouragement of this work. We thank Mr. Siju, Mr. V. Praveen Kumar and Smt. S. Latha for recording FESEM, 3D roughness and image analysis software, respectively.

References

[1] T. Verho, C. Bower, P. Andrew, S. Franssila, O. Ikkala, R. H. A. Ras, *Adv. Mater.* **2011**, *23*, 673.
[2] C. Y. Peng, S. L. Xing, Z. Q. Yuan, J. Y. Xiao, C. Q. Wang, J. C. Zeng, *Appl. Surf. Sci.* **2012**, *259*, 764.
[3] T. Bharathidasan, S. V. Kumar, M. S. Bobji, R. P. S. Chakradhar, B. J. Basu, *Appl. Surf. Sci.* **2014**, *314*, 241.
[4] C. K. Soz, E. Yilgor, I. Yilgor, *Polymer.* **2015**, *62*, 118.
[5] H. Tada, H. Nagayama, *Langmuir.* **1995**, *11*, 136.
[6] A. Nakajima, K. Hashimoto, T. Watanabe, *Monatsh Chem.* **2001**, *132*, 31.
[7] R. Blossey, *Nat. Mater.* **2003**, *2*, 301.
[8] G. Gu, H. Dang, Z. Zhang, Z. Wu, *Appl. Phys. A.* **2006**, *83*, 131.
[9] P. N. Manoudis, I. Karapanogiotis, A. Tsakalof, I. Zuburtikudis, C. Panayiotou, *Langmuir.* **2008**, *24*, 11225.
[10] S. H. Lee, H. S. Han, K. S. Han, J. H. Shin, S. Y. Hwang, H. Lee, *Prog. Photovoltaics.* **2013**, *21*, 1056.
[11] W. H. Haung, C. S. Lin, *Appl. Surf. Sci.* **2014**, *305*, 702.
[12] X. J. Liu, Y. Xu, K. Y. Ben, Z. Chen, Y. Wang, Z. S. Guan, *Appl. Surf. Sci.* **2015**, *339*, 94.
[13] S. C. Guo, F. Wu, L. Fang, C. Y. Mao, Y. Y. Dou, *Mater. Tech.* **2015**, *30*, 43.
[14] R. P. S. Chakradhar, V. D. Kumar, J. L. Rao, B. J. Basu, *Appl. Surf. Sci.* **2011**, *257*, 8569.
[15] R. P. S. Chakradhar, V. D. Kumar, C. Shivakumara, J. L. Rao, B. J. Basu, *Surf., Interf. Anal* **2012**, *44*, 412.
[16] R. P. S. Chakradhar, G. Prasad, P. Bera, C. Anandan, *Appl. Surf. Sci.* **2014**, *301*, 208.
[17] H. Lu, X. Xu, Z. Li, Z. Zhang, *Bull Mater. Sci.* **2006**, *29*, 485.
[18] C. Ramesh, *Macromolecules.* **1999**, *32*, 5704.
[19] K. Inoue, S. Hoshino, J. Polym, *Sci., B: Polym. Phys.* **1973**, *11*, 1077.
[20] N. Hiramatsu, K. Haraguchi, S. Hirakawa, S. Jpn, *J. Appl. Phys.* **1982**, *21*, 335.
[21] E. Stamhuis, A. Pennings, *J. Polymer.* **1977**, *18*, 667.
[22] S. Rhee, J. L. White, J. Polym, *Sci., B: Polym. Phys.* **2002**, *40*, 1189.
[23] S. Music, N. Filipovic-Vincekovic, L. Sekovanic, *Brazilian J. Chem. Eng.* **2011**, *28*, 89.
[24] G. Nallathambi, T. Ramachandran, V. Rajendran, R. Palanivelu, *Mater. Res.* **2011**, *14*, 552.
[25] D. Y. Wang, H. Mohward, *Adv. Mater.* **2004**, *16*, 244.
[26] P. Jiang, M. J. McFarland, *J. Am. Chem. Soc.* **2004**, *126*, 13778.
[27] A. Nakajima, *J. Ceram. Soc. Jp.* **2004**, *112*, 533.
[28] Y. Guo, Q. Wang, T. Wang, *J. Mater. Sci.* **2011**, *46*, 4079.
[29] R. V. Lakshmi, T. Bharathidasan, P. Bera, B. J. Basu, *Surf. Coat. Technol.* **2012**, *206*, 3888.
[30] C. J. Powell, P. E. Larson, *Appl. Surf. Sci.* **1978**, *1*, 186.
[31] J. H. Scofield, J. Electron, *Spectrosc. Relat. Phenom.* **1976**, *8*, 129.
[32] D. R. Penn, J. Electron, *Spectrosc. Relat. Phenom.* **1976**, *9*, 29.
[33] a J. P. Bange, L. S. Patil, D. K. Gautam, *Progress in Electromag. Res.b* ▪▪▪, *3*, 165.
[34] a A. S. Luyt, I. Krupa, H. J. Assumption, E. E. M. Ahmad, J. P. Mofokeng, *Polym.bTest* **2010**, *29*, 100.
[35] R. N. Wenzel, *Ind. Eng. Chem.* **1936**, *28*, 988.
[36] A. B. D. Cassie, S. Baxter, *Trans Faraday Soc.* **1944**, *40*, 546.
[37] P. Roach, N. J. Shirtcliffe, M. I. Newton, *Soft Matter.* **2004**, *4*, 22.
[38] T. Young, *Phil. Trans. R. Soc. (London),* **1805**, *95*, 65.
[39] A. Dupre, *Theorie Mecanique de la Chaleur*, Paris, **1869**.
[40] X. T. Zhang, H. Kono, Z. Y. Liu, S. Nishimoto, D. A. Tryk, T. Murakami, H. Sakai, M. Abeb, A. Fujishima, *Chem. Commun.* **2007**, *46*, 4949.

Author Query Form

Journal: Surface and Interface Analysis

Article: sia_6175

Dear Author,

During the copyediting of your paper, the following queries arose. Please respond to these by annotating your proofs with the necessary changes/additions.

- If you intend to annotate your proof electronically, please refer to the E-annotation guidelines.
- If you intend to annotate your proof by means of hard-copy mark-up, please use the standard proofing marks. If manually writing corrections on your proof and returning it by fax, do not write too close to the edge of the paper. Please remember that illegible mark-ups may delay publication.

Whether you opt for hard-copy or electronic annotation of your proofs, we recommend that you provide additional clarification of answers to queries by entering your answers on the query sheet, in addition to the text mark-up.

Query No.	Query	Remark
Q1	AUTHOR: We have provided "Transparent hydrophobic and superhydrophobic coatings" as the "Running head" for this article. It will appear on the top of the third page and all the recto pages of the article. Please confirm if this is appropriate.	
Q2	AUTHOR: Please confirm that given names (red) and surnames/family names (green) have been identified correctly.	
Q3	AUTHOR: Kindly check data here and revise for clarity if necessary: …addition of more layers results in a slight decrease in the surface roughness, agglomeration of silica particles which resulted in a slight decrease in WCA.	

WILEY

USING e-ANNOTATION TOOLS FOR ELECTRONIC PROOF CORRECTION

Required software to e-Annotate PDFs: Adobe Acrobat Professional or Adobe Reader (version 7.0 or above). (Note that this document uses screenshots from Adobe Reader X)
The latest version of Acrobat Reader can be downloaded for free at: http://get.adobe.com/uk/reader/

Once you have Acrobat Reader open on your computer, click on the Comment tab at the right of the toolbar:

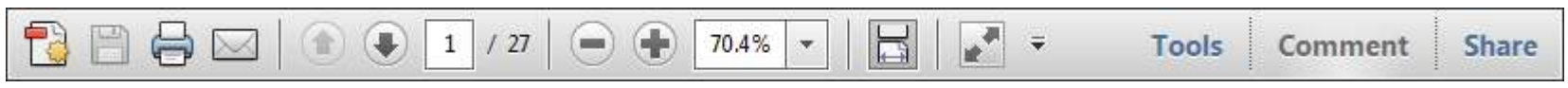

This will open up a panel down the right side of the document. The majority of tools you will use for annotating your proof will be in the Annotations section, pictured opposite. We've picked out some of these tools below:

1. Replace (Ins) Tool – for replacing text.

Strikes a line through text and opens up a text box where replacement text can be entered.

How to use it

- Highlight a word or sentence.
- Click on the Replace (Ins) icon in the Annotations section.
- Type the replacement text into the blue box that appears.

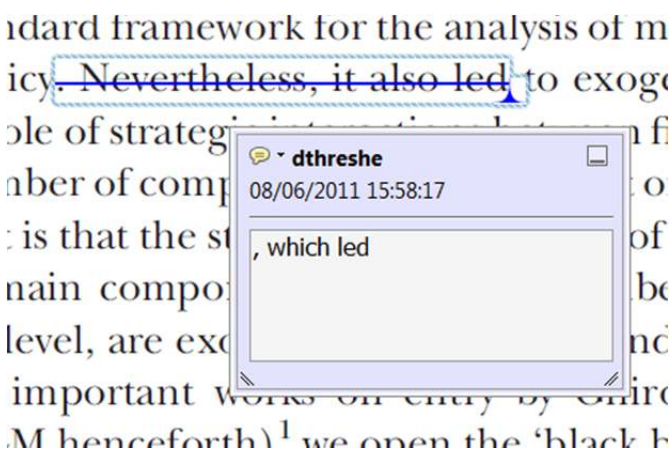

2. Strikethrough (Del) Tool – for deleting text.

Strikes a red line through text that is to be deleted.

How to use it

- Highlight a word or sentence.
- Click on the Strikethrough (Del) icon in the Annotations section.

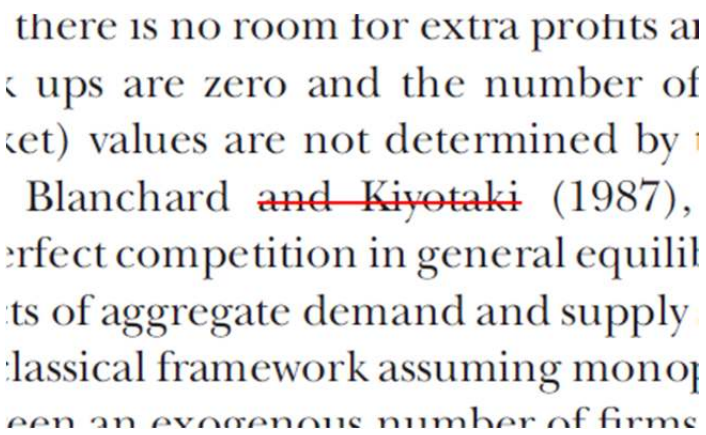

3. Add note to text Tool – for highlighting a section to be changed to bold or italic.

Highlights text in yellow and opens up a text box where comments can be entered.

How to use it

- Highlight the relevant section of text.
- Click on the Add note to text icon in the Annotations section.
- Type instruction on what should be changed regarding the text into the yellow box that appears.

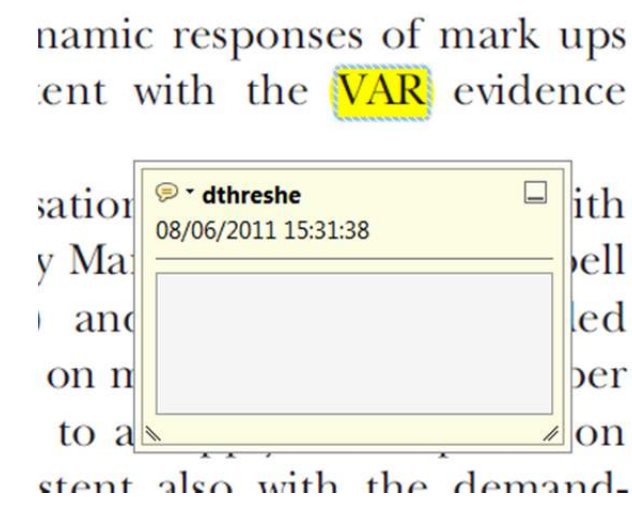

4. Add sticky note Tool – for making notes at specific points in the text.

Marks a point in the proof where a comment needs to be highlighted.

How to use it

- Click on the Add sticky note icon in the Annotations section.
- Click at the point in the proof where the comment should be inserted.
- Type the comment into the yellow box that appears.

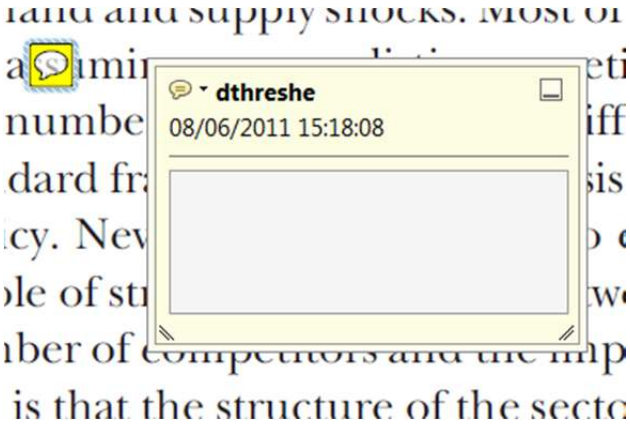

WILEY

USING e-ANNOTATION TOOLS FOR ELECTRONIC PROOF CORRECTION

5. Attach File Tool – for inserting large amounts of text or replacement figures.

Inserts an icon linking to the attached file in the appropriate pace in the text.

How to use it

- Click on the Attach File icon in the Annotations section.
- Click on the proof to where you'd like the attached file to be linked.
- Select the file to be attached from your computer or network.
- Select the colour and type of icon that will appear in the proof. Click OK.

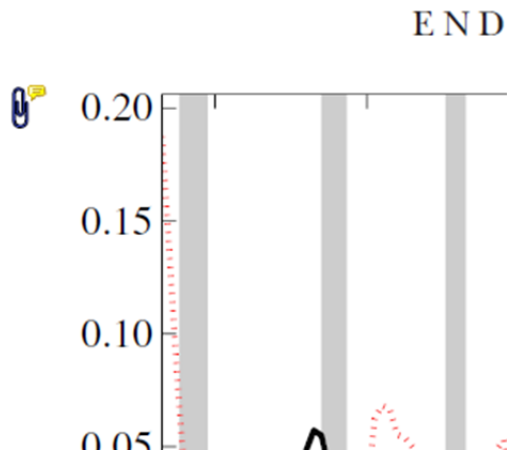

6. Add stamp Tool – for approving a proof if no corrections are required.

Inserts a selected stamp onto an appropriate place in the proof.

How to use it

- Click on the Add stamp icon in the Annotations section.
- Select the stamp you want to use. (The Approved stamp is usually available directly in the menu that appears).
- Click on the proof where you'd like the stamp to appear. (Where a proof is to be approved as it is, this would normally be on the first page).

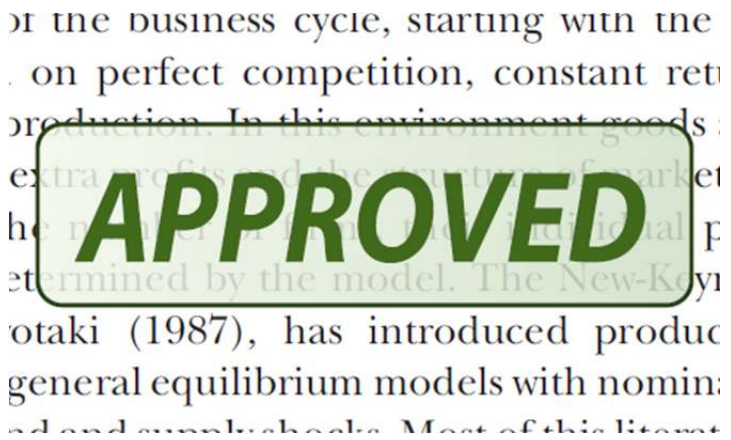

7. Drawing Markups Tools – for drawing shapes, lines and freeform annotations on proofs and commenting on these marks.

Allows shapes, lines and freeform annotations to be drawn on proofs and for comment to be made on these marks..

How to use it

- Click on one of the shapes in the Drawing Markups section.
- Click on the proof at the relevant point and draw the selected shape with the cursor.
- To add a comment to the drawn shape, move the cursor over the shape until an arrowhead appears.
- Double click on the shape and type any text in the red box that appears.

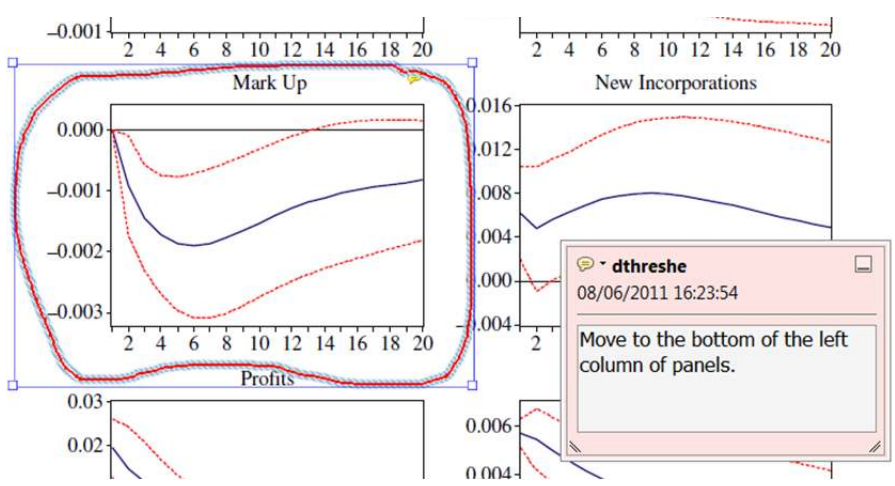

For further information on how to annotate proofs, click on the Help menu to reveal a list of further options: